Science Advances
AAAS

advances.sciencemag.org/cgi/content/full/5/6/eaav7686/DC1

Supplementary Materials for

Tuning from failed superconductor to failed insulator with magnetic field

Yangmu Li, J. Terzic, P. G. Baity, Dragana Popović, G. D. Gu, Qiang Li, A. M. Tsvelik, J. M. Tranquada*

*Corresponding author. Email: jtran@bnl.gov

Published 14 June 2019, *Sci. Adv.* **5**, eaav7686 (2019)
DOI: 10.1126/sciadv.aav7686

This PDF file includes:

Estimation of *c*-axis misorientation for sample B
Fig. S1. Temperature-magnetic field phase diagram for A2.
Fig. S2. Field dependence of Hall voltage at various temperatures.
Fig. S3. Sheet resistance at constant magnetic field.
Fig. S4. ac nonlinear resistivity at H_{2D} for various temperatures.
Fig. S5. Additional results for sample B.
Fig. S6. Comparison between A1 and previous results for a similar sample.

Estimation of *c*-axis misorientation for sample B

The *c*-axis misorientation in sample B can be estimated based on the zero-field resistivities of samples A and B, and the previous measurement of ρ_c in Ref. 14, all at T = 40 K. We have ρ_A = 0.5 mΩ cm ≈ ρ_{ab}, ρ_B = 1.05 mΩ cm, and ρ_c = 800 mΩ cm. Solving Laplace's equation for the anisotropic resistivity tensor assuming a small misalignment angle α, we obtain

$$\rho_B = \rho_{ab}\cos^2\alpha + \rho_c\sin^2\alpha \approx \rho_{ab} + \rho_c\alpha^2$$

Hence, we find that $\alpha = \sqrt{(\rho_B - \rho_A)/\rho_c} \approx 0.026$, which corresponds to 1.5°.

We can also invert the formula in order to estimate the resistivity anisotropy at high field. We find: $\rho_c/\rho_{ab} \approx [(\rho_B/\rho_A) - 1]/\alpha^2$. We are interested in the anisotropy ratio in the UQM state at 35 T. We have to pick a temperature where R_s of A1 is saturated, and take T = 3.0 K. Then from Fig. 3, we find that R_s values for A1 and B are 1.93 R_Q and 2.03 R_Q, respectively. This yields $\rho_c/\rho_{ab} \approx 77 < 10^2$. We note a 10 percent uncertainty in the measurement of sample dimensions. Taken this effect to its extreme, assuming ρ_A = 0.9 x 1.93 R_Q and ρ_B = 1.1 x 2.03 R_Q, we obtain $\rho_c/\rho_{ab} \approx 391$, still much less than the nominal resistivity anisotropy ~ 10^4 at zero field.

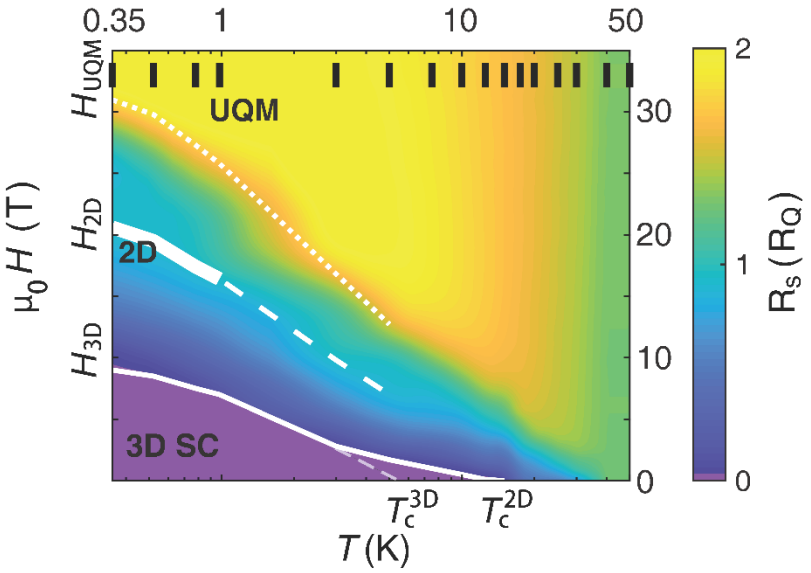

Fig. S1. Temperature-magnetic field phase diagram for A2. Temperature-magnetic field phase diagram for A2 plotted with the identical method as that for A1 (Fig. 1A). Color map indicates the magnitude of R_s. Solid, dashed, and dotted white lines show H_{3D}, H_{2D} and H_{UQM}, respectively. Black bars at top indicate temperatures of measurements used to produce the phase diagram. A progression from 3D superconducting order, through a 2D order, to the ultra-quantum metal state is observed as a function of magnetic field. The characteristic fields H_{3D}, H_{2D} and H_{UQM}, are identical to those for A1. The phase diagram for A1 (Fig. 1A) and A2 (fig. S1) are almost identical, except in the 2D SC regime. The broad white band indicates where $R_s \approx R_Q$ for A2, which is in the exact same region where 2D superconductivity is observed for A1 (Fig. 1A). $R_s \approx 2R_Q$ is observed in the ultra-quantum metal state for both A1 and A2. At higher temperatures, R_s for A1 and A2 lose quantization at $H = H_{2D}$ simultaneously.

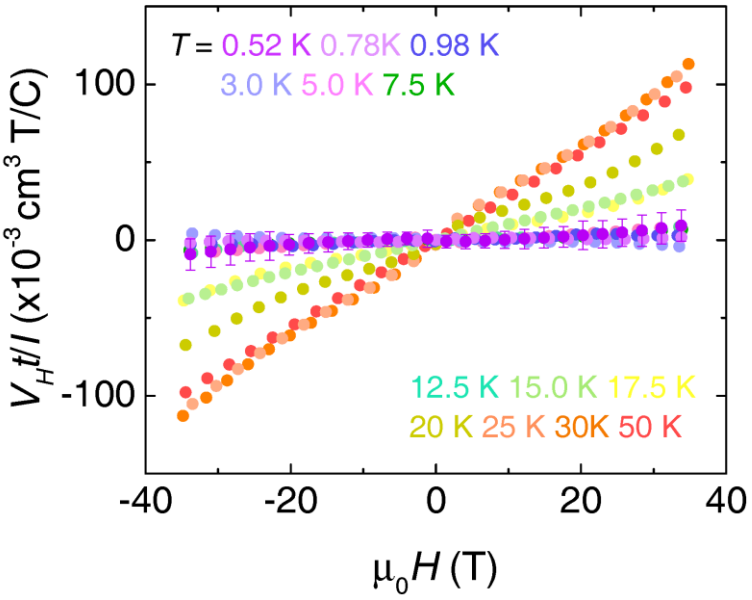

Fig. S2. Field dependence of Hall voltage at various temperatures. Hall voltage plotted as $V_H t/I$ versus magnetic field for all measured temperatures, where V_H is the Hall voltage, t is the sample thickness, and I is the current, respectively. Data are binned and antisymmetrized to remove the longitudinal magnetoresistance contribution that results from slight mis-alignment of voltage contacts. The nonlinear dependence on field comes from an imperfect cancellation of the longitudinal magnetoresistance contribution. Example of error bars due to noise are plotted for T = 0.52 K. Hall coefficient is obtained by a linear fit of the data for $|\mu_0 H| < 10$ T. The error bars shown in Fig. 1B come from the spread in values of R_H obtained over the entire field range, for a given temperature. Below 15 K, the Hall voltage is effectively zero. To put the magnitude of the low temperature response in perspective, consider the case of T = 0.52 K and field of 34 T; the value of R_H there is $2.8 \pm 3.0 \times 10^{-4}$ cm^3/C. If we were to interpret this value as being due to fermionic quasiparticles, we would end up with a hole concentration of 2.1, which is not physically realistic. For comparison, the Hall coefficient for LBCO with x = 0.095 was measured previously in Ref. 17 for the same range of magnetic field. At low magnetic fields, our results for LBCO with x = 0.125 (Fig. 1B) are similar to those for LBCO with x = 0.095, but with a lower superconducting transition temperature.

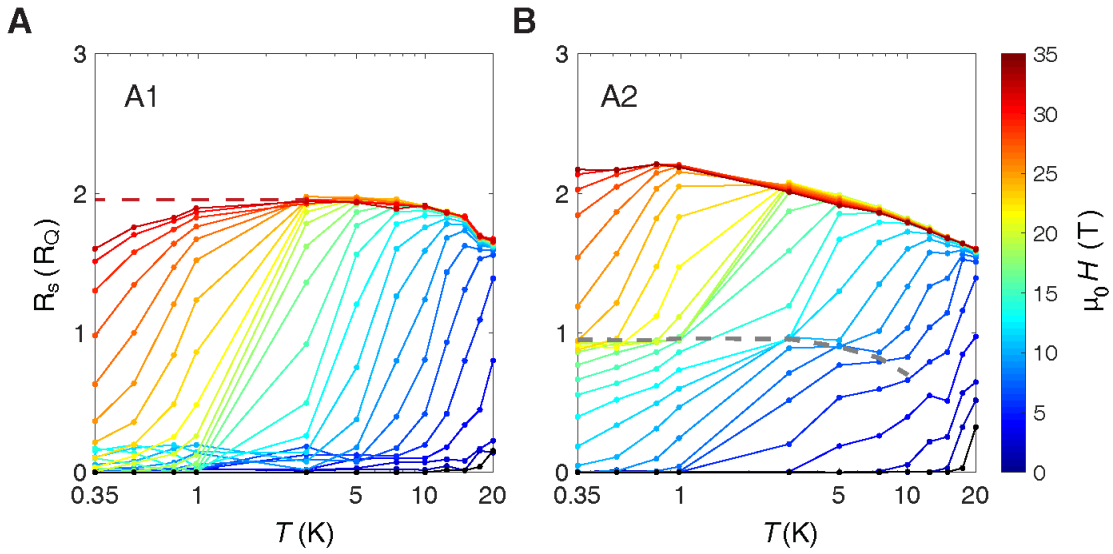

Fig. S3. Sheet resistance at constant magnetic field. Sheet resistance of A1 (**A**) and A2 (**B**) vs. temperature at constant magnetic field, converted from data obtained by field sweeps, plotted in semi-log format. Color-coded solid lines indicate constant fields. The reentrant 2D superconductivity is visible in the figure for A1 and the corresponding quantization of $R_S \approx R_Q$ is indicated by a dashed grey band in the figure for A2. Dashed line for A1 indicates the saturation of resistivity at magnetic field slightly higher than 35 T, as obtained by extrapolating the scaling behavior apparent in Fig. 3D and E.

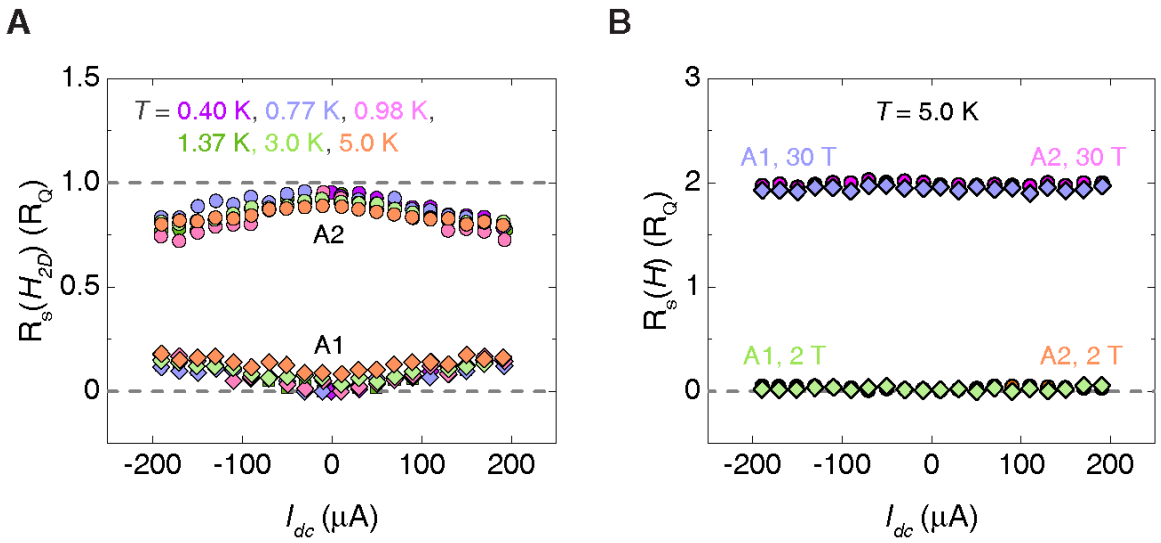

Fig. S4. ac nonlinear resistivity at H_{2D} for various temperatures. (**A**) *ac* nonlinear resistivity at H_{2D} for all measured temperatures, $0.4 \leq T \leq 5$ K. The data at T = 0.98 K are included in Fig. 4C. R_s (H_{2D}) for A1 becomes non-zero at high *dc* current, while that for A2 deviates downwards from R_Q. At temperatures above 1 K, $R_s(H_{2D})$ for both A1 and A2 lose quantization even at lowest dc current (also shown in Fig. 4A, B). Data were taken at fields of 20 T, 17.5 T, 15 T, 13T, 9 T, and 6 T for T = 0.40 K, 0.77 K, 0.98 K, 1.37 K, 3.0 K, and 5.0 K, respectively. (**B**) *ac* resistivity at 2 T (below H_{3D}) and 30 T (above H_{UQM}) for T = 5 K. At both fields, *ac* resistivity is independent of the *dc* currents, in contrast to the nonlinear resistivity at H_{2D} in (A) and in Fig. 4C.

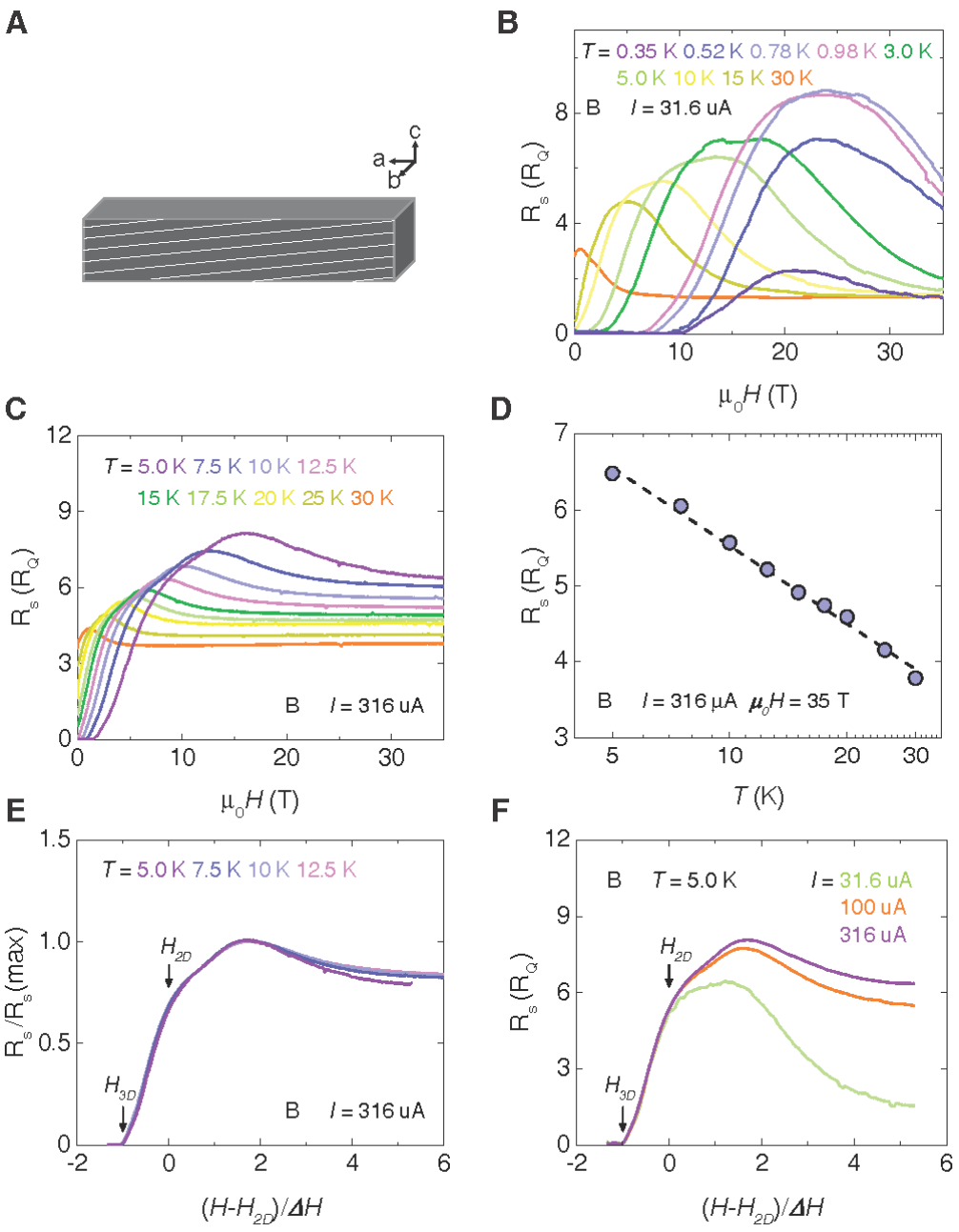
A
c
a
b
B
T = 0.35 K 0.52 K 0.78 K 0.98 K 3.0 K
5.0 K 10 K 15 K 30 K
B I = 31.6 uA
R_s (R_Q)
μ_0H (T)
C
T = 5.0 K 7.5 K 10 K 12.5 K
15 K 17.5 K 20 K 25 K 30 K
B I = 316 uA
R_s (R_Q)
μ_0H (T)
D
B I = 316 μA μ_0H = 35 T
R_s (R_Q)
T (K)
E
T = 5.0 K 7.5 K 10 K 12.5 K
H_2D
H_3D
B I = 316 uA
R_s/R_s (max)
(H-H_2D)/ΔH
F
B T = 5.0 K
I = 31.6 uA
100 uA
316 uA
H_2D
H_3D
R_s (R_Q)
(H-H_2D)/ΔH

Fig. S5. Additional results for sample B. (**A**) Schematic illustration of *c*-axis misorientation for sample B; white lines indicate CuO_2 planes. (**B**) R_s at various temperatures with I = 31.6 μA. R_s at 0.35 K decreases to a magnitude that is comparable to sample A1 and A2. (**C**) R_s at various temperatures with I = 316 μA, 10 times that shown in Fig. 3C. The R_s at high magnetic field and high current shows a non-metallic behavior, different from that at low current (Fig. 3C). (**D**) Semi-log plot of R_s at 15 T with I = 316 μA. The dashed line indicates the logarithmic temperature dependence. (**E**) Data same as in (C) but with the magnetic field scaled as in Fig. 3D-F. The magnitude of R_s is also normalized to the maximum value. The effect of temperature at high field is similar to that of the current. (**F**) R_s for various currents at T = 5 K. A dramatic difference of R_s is observed only for $H > H_{2D}$, in sharp contrast to the effect of current on A1 and A2 (Figs. 4 and S4).

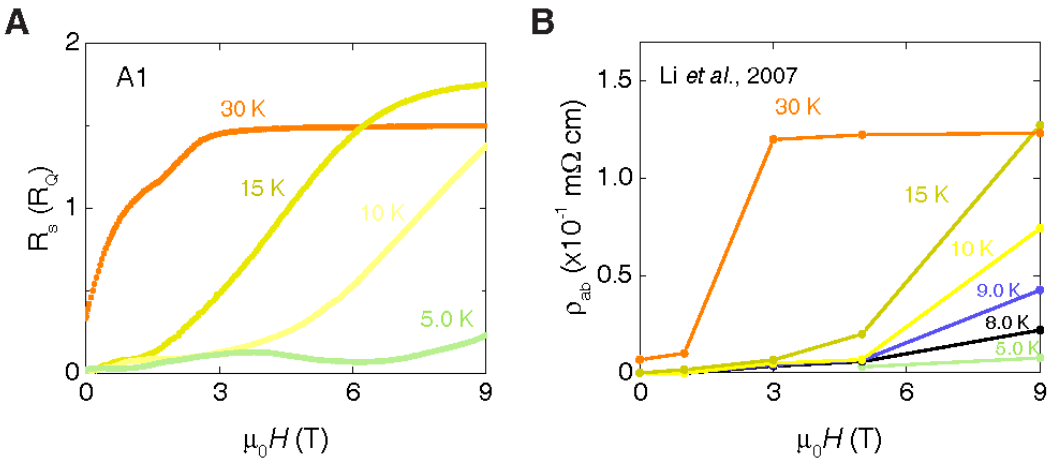

Fig. S6. Comparison between A1 and previous results for a similar sample. (**A**) Sheet resistance as a function of magnetic field (below 9 T) of sample A1 for selected temperatures. The data for the full field range are included in Fig. 3A. R_s was measured with an *ac* current of 31.6 μA. (**B**) In-plane resistivity vs. magnetic field previously reported for a related sample. The data at 0 T, 1 T, 3 T, 5 T, and 9 T are obtained from constant field measurements in Ref. 14 with a current much larger than 31.6 μA. We note that, on converting to the same units, the resistivity magnitude is somewhat different for the two measurements, as it is sensitive to precise Ba and O concentrations and to measurements of the sample dimensions. Despite the differences between currents used and between data densities, an overall similarity is observed for the two samples.